Journal of Electroceramics 6:1, 43–54, 2001

Modified Citrate Gel Techniques to Produce ZnO-Based Varistors (Part I—Microstructural Characterisation)

A. LORENZ, J. OTT, M. HARRER, E.A. PREISSNER, A.H. WHITEHEAD & M. SCHREIBER
Christian Doppler Laboratory for Hybrid Materials, Austrian Research Center Seibersdorf, A-2444 Seibersdorf, Austria

Submitted April 20, 2000; Revised June 30, 2000; Accepted September 12, 2000

Abstract. Two novel chemical processing routes were developed for the production of ZnO-based varistor powders and compared with the conventional mixed-oxide route. The central idea behind the new techniques was to separate the minority components in relation to their function and incorporate them into the varistor powders accordingly. The densification of green bodies prepared by the chemical routes proceeded in one or two stages (at 770 °C and 910 °C) compared to many stages for the conventional route. The sintered pellets thus produced from the chemical routes showed smaller grain sizes, higher densities and more evenly distributed intergranular phases than those from the conventional mixed-oxide route.

Keywords: zinc oxide varistors, ZnO, citrate gel process, microstructure

1. Introduction

The non-linear electrical properties of ZnO varistors are determined by grain boundary phenomena [1]. The nature of the grain boundaries are, in turn, governed by the precursor powder composition and the sintering and cooling conditions [2]. Commercial ZnO varistors compositions typically comprise minor quantities of ten to twenty different oxides [3] (including Bi_2O_3, Sb_2O_3, CoO, MnO, Cr_2O_3, SiO_2) which influence the grain growth [4–6], the grain conductivity [7] or which act as flux in the liquid-phase sintering process [4–6]. In accordance with common usage, they shall be referred to here as dopants (grain conductivity enhancers) and additives (grain boundary formers).

Most commercial ZnO varistors are prepared by a fabrication technique which is known as the solid-state mixed-oxide route [8]. Several problems are associated with the mixed-oxide route. Because the ZnO, dopants and additives are typically mixed together as fine particles using a ball mill, inhomogeneities in the resulting powder cannot be completely avoided. Compositional and particle size inhomogeneities are dependent on the exact milling conditions. A uniform spatial distribution of the starting oxides is hard to obtain, especially when one oxide is present in small amounts, as is normally found for the dopants. Furthermore, impurities due to abrasion from the milling equipment (wall and balls) render the situation even more complex. As a consequence of large particle size distributions and low diffusion coefficients of the oxides, high sintering temperatures and long sintering times are required to obtain satisfactory varistor pellets. However, doping by the solid-state route can still lead to inhomogeneous grains after sintering.

Our ultimate goal was to develop a processing route to fabricate high-voltage/ high-power varistors. A homogeneous microstructure, with controlled ZnO grain size and with a narrow particle-size distribution, may be assumed as a pre-requisite for these characteristics. A further requisite would be the even distribution of additives along the grain boundaries. Chemical preparation techniques were viewed as potentially the best means to synthesize samples with these properties. This view was encouraged, in part, by the report of Santhosh *et al* [9] that a liquid-phase chemical synthesis route could be used to produce SnO_2-based

Current address: Funktionswerkstoffe F & E GmbH, Marktstrasse 3, A-7000 Eisenstadt, Austria

varistors with significantly improved properties over the conventional ceramic route.

Dosch *et al.* [10] describe a process for ZnO varistor powder synthesis in which a co-precipitation process from chlorides was used. An interesting feature of this approach is related to the sequence of precipitation of the various constituents. The strategy employed was to separate the manufacturing process into several steps and to use the constituents in the appropriate step based on their later functionality. In this respect, the dopants were co-precipitated with ZnO, since they were required within the grains to enhance the electrical conductivity. After a calcination step, additives were precipitated onto the surface of the doped ZnO grains. The additives are mostly responsible for the intergranular Schottky barrier formation and were also required to provide the flux for the liquid-phase sintering process. Related precipitation procedures are described by Haile [11] and Westin [12,13]. In these cases pure ZnO was covered by a coating of dopant and additive oxides.

The preparation of relatively pure mixed metal oxides by pyrolysis of citrate precursors has been known for some time [14]. Fan [3] demonstrated that a single step citrate gel route could be used to prepare ZnO varistors with increased nonlinearity coefficients and high characteristic breakdown voltages. Other studies have been reported, in which the citrate gel process has been employed successfully to prepare a range of substituted perovskite oxides [15,16], superconductors [17] and soft-ferrite powders [18]. The citrate gel process produces a solid amorphous precursor material by dehydration of citrate gels which are formed through the addition of citric acid to an aqueous solution containing nitrate salts of the relevant metals.

Citric acid is an α-hydroxy tricarboxylic acid which has two different functional groups: the α-hydroxy group acts in combination with one carboxylate group as a complexing ligand to bind the metal cations (Fig. 1a). The uncoordinated carboxylic groups of the citric acid can be used to anchor the five-membered chelate ring on the surface of the ZnO-grain (Fig. 1b). The bonding of citric acid to the surface of ZnO also leads to a dispersion effect which prevents agglomeration of the ZnO particles in solution.

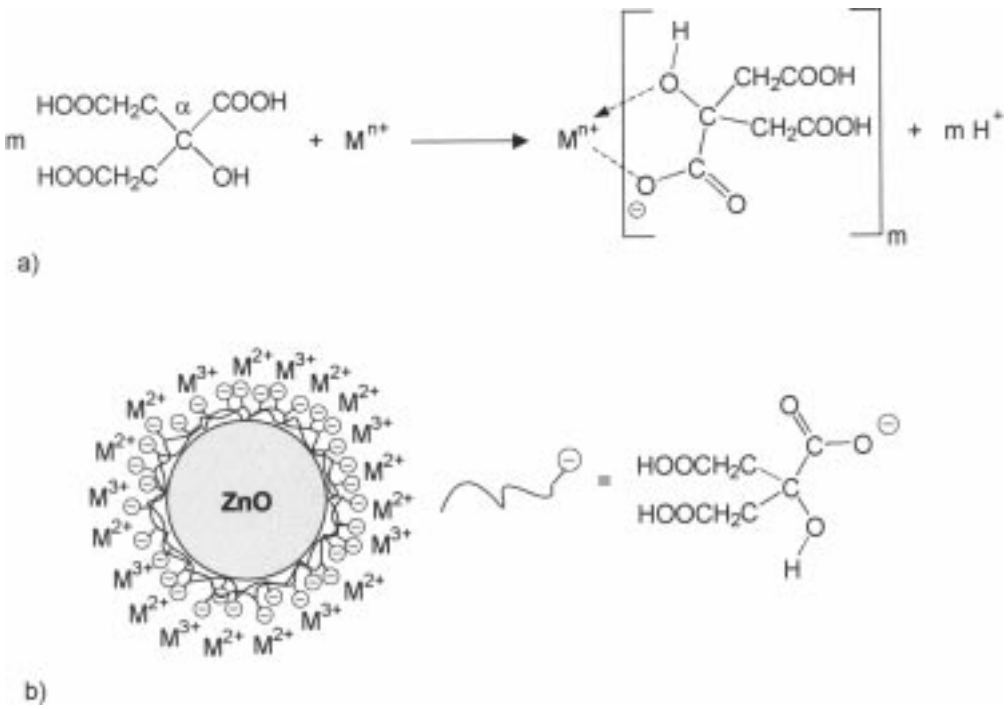

Fig. 1. The action of citric acid in the precipitation routes; a) the co-ordination of citric acid to metal ions, b) schematic representation of the action of citric acid in precipitation of metal ions onto ZnO particles.

The citrate gel method offers several advantages over other techniques, including:

- unwanted precipitation does not occur during gel manufacture
- separation of the components is prevented due to the high viscosity of the solution
- the homogeneity of the aqueous solution of salts is preserved in the gel and possibly into the final solid oxide product
- simplicity of the basic chemistry and processes needed for the production of the powder

In this work the citrate gel process was combined with the strategies of co-precipitation employed by Dosch [10] and precipitation by Westin [12,13] to prepare ZnO-based varistors. However, the citrate-gel process described above was modified by using acetates instead of nitrates of the relevant metals (except for Bi and Al for which nitrates were used). Acetates were preferred over nitrates as they produced less toxic side products during powder calcination.

As a reference material, varistor samples of the same composition were prepared by the conventional mixed-oxide route.

2. Experimental Procedure

Varistors composed of the following were prepared: ZnO with Co, Mn, Al, Ni, and Cr dopants, and Bi, Sb, Ba, Si, and B additives. The total amount of dopants and additives equalled 7 at%. The precursors for the powder preparation were: sub-micron pharmaceutical grade ZnO, citric acid, $Co(OAc)_2.4H_2O$, $Mn(OAc)_2.4H_2O$, $Al(NO_3)_3.9H_2O$, $Ni(OAc)_2.4H_2O$, $Cr_3(OAc)_7(OH)_2$, $Bi(NO_3)_3.5H_2O$, $Sb(OAc)_3$, $Ba(OAc)_2$, H_3BO_3, $Si(OEt)_4$, and 5 N NH_4OH solution.

A schematic representation of the three synthetic routes is shown in Fig. 2 and a more detailed description given below.

Route 0

The conventional mixed-oxide route, used to prepare reference samples, is denoted as route 0. Powders prepared by this route (ball milling of the additive and dopant oxides with ZnO) were obtained from Siemens-Matsushita.

Route 1

The novel synthetic processes (denoted route 1 and route 2) were adapted after the procedures described by Dosch [10] and Westin [12,13]. Both routes consisted of two steps. In the first step a doped ZnO powder was prepared. For route 1 this was achieved by coating a ZnO powder with a layer of citrates of the dopants using the citrate-gel technique. Explicitly, individual solutions of each precursor material were made by dissolving the relevant dopant metal salts (Co, Mn, Al, Ni, Cr) in aqueous citric acid solution. The molar ratio of citric acid to each salt is given in Table 1. Given amounts of the citrate solutions of each dopant were added sequentially to a suspension of ZnO powder in de-ionised water.

The suspension was stirred with a sawtooth mixer for up to 18 h and then dehydrated using a rotary evaporator at temperatures up to 70 °C under reduced pressure (20–30 mbar) until a dry powder was obtained. The powder was then placed in a drying oven at 70 °C overnight to remove residual water. The coated ZnO powder was then calcined at 480 °C for 4 h (heating rate: 3 °C min^{-1}, cooling rate: 3 °C min^{-1}) in order to remove the organic components and to encourage diffusion of the dopants throughout the ZnO grains.

In the second step the doped ZnO powder was coated with a layer of the additives. Citrate solutions of the additives were prepared in the following ways. The barium and boron salts were dissolved in citric acid with a minimum amount of water. $Si(OEt)_4$ was diluted in ethanol. Antimony acetate was added directly to the citric acid and stirred vigorously for about 30 min. The bismuth salt, $Bi(NO_3)_3.5H_2O$, was added to a solution containing 10 mole equivalents of citric acid. A solution of 5 mol dm^{-3} NH_4OH was added dropwise under vigorous stirring until a pH value of 7 was achieved, coinciding with complete dissolution of the salt. The molar ratios of citrate to the additive salts are given in Table 2.

The doped ZnO powder was added to a reaction vessel containing the bismuth salt solution, which was stirred continuously. Subsequently, the citrate solutions of the other additives were transferred sequentially to the reaction vessel and the resulting suspension stirred for about 18 h. The liquid phase (solvent)

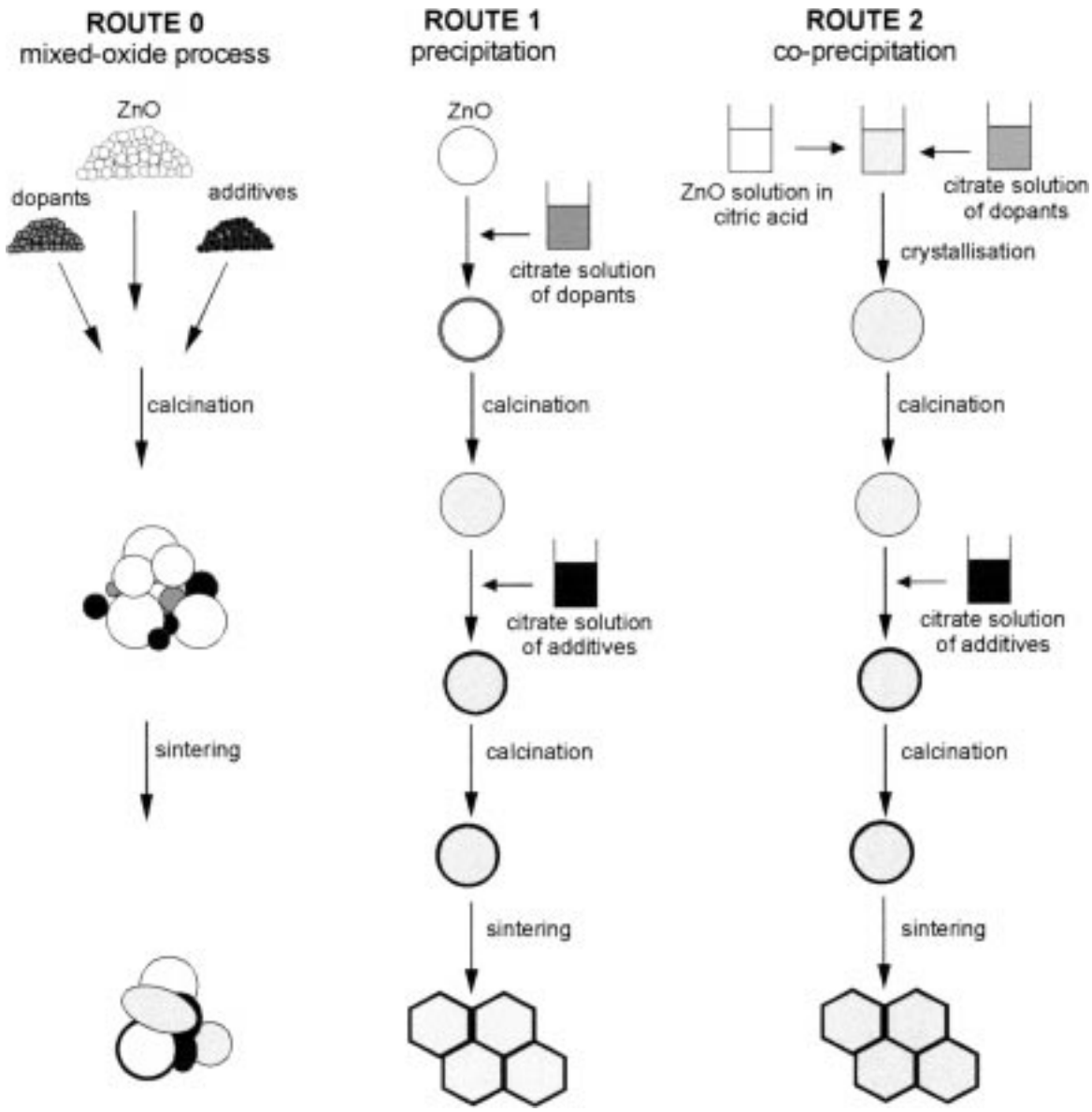

Fig. 2. Schematic representation of the three methods to synthesis doped ZnO varistor pellets.

Table 1. Molar ratio of citric acid to dopant

Metal salt	$Co(OAc)_2.4H_2O$	$Mn(OAc)_2.4H_2O$	$Al(NO_3)_3.9H_2O$	$Ni(OAc)_2.4H_2O$	$Cr_3(OAc)_7.(OH)_2$
Molar ratio of citrate:dopant	2:1	2:1	3:1	2:1	9:1

Table 2. Molar ratio of citric acid to additive

Metal salt	$Bi(NO_3)_3.5H_2O$	$Sb(OAc)_3$	$Ba(OAc)_2$	H_3BO_3	$Si(OEt)_4$
Molar ratio, citrate:additive	10:1	4:1	2:1	3:1	4:1

was removed completely in a rotary evaporator under reduced pressure to yield a solid material which was calcined under an ambient atmosphere at 480 °C for 4 h (heating rate: 3 °C min^{-1}, cooling rate 3 °C min^{-1}) to form the oxide powder. This second calcination step led to doped ZnO powders which were coated with a layer of additive oxides.

Route 2

As for the route 1 method a doped ZnO powder was produced initially. The doped powder was prepared by co-precipitation of zinc citrate and citrates of the dopants from an aqueous solution. Commercial available ZnO powder was completely dissolved in an excess of citric acid (three mole equivalents of citric acid). The influence of varying the ratio of citric acid to ZnO on the particle properties of doped ZnO will be the topic of a further paper. Individual citrate solutions of the dopants, as described above for route 1, were added to the clear, colourless zinc-citrate solution. After stirring for about 30 min the solution was dehydrated in a rotary evaporator under reduced pressure (20–30 mbar) and up to 70 °C to produce a highly viscous gel. Crystallisation of the gel occurred by ageing for 16 h at room temperature or slightly above (20–50 °C). The citrate powder was then calcined in air at 480 °C for 4 h to remove the organic components.

The co-precipitation technique used in route 2 was anticipated to provide the most homogeneous distribution of dopants in the ZnO grains as the homogeneity was incorporated initially in the precursor powder.

The second step of route 2, to coat the doped ZnO powder with a layer of additives, was identical to that described for route 1 above.

Compaction and Sintering

The powders from routes 0, 1 and 2 were individually ground with a pestle and mortar. Each powder was then granulated with the addition of an organic binder mixture (2%), obtained from Siemens-Matsushita. The granules were dried and sieved prior to palletising. 400 mg of a given powder was uniaxial pressed to form each 10 mm diameter pellet.

After thermal removal of the binder at 400 °C green bodies were formed. Using a dilatometer, measurements of the normalised change in sample thickness (linear expansion, $\Delta L/L_o$) were made with increasing temperature (heating rate 3 °C min^{-1} in air) on green bodies prepared by the three routes. The differential length change with temperature (differential linear expansion, $d(\Delta L)/dT$) was also calculated. Sintered pellets were prepared from the green bodies by heating in air to 1000 °C for 90 min (heating rate 3 °C min^{-1}, cooling rate 1 °C min^{-1}) which yielded dark grey ceramic bodies of approximately 1.2 mm thickness. The sintered pellets formed by routes 0, 1 and 2 were denoted P0, P1 and P2 respectively.

Microstructural Observation

The distribution of the intergranular phase of each sintered and polished specimen was observed by scanning electron microscopy (SEM) with a backscattered electron (BSE) detector (Zeiss DSM 950). Thermal etching of the polished samples (20 min at 800 °C) was used to elucidate the microstructure and grain size of each specimen when using SEM with a secondary electron (SE) detector. The accelerating voltage was 20 KeV and the magnification 1000 × in each instance.

3. Results and Discussion

As shown in Figs. 3 to 5, by the differential linear expansion with temperature, the green bodies from routes 1 showed a slightly earlier onset of densification than for routes 0 and 2 (680 °C compared with 730–750 °C, respectively). However, more strikingly the densification of materials from routes 1 and 2 was largely complete (the magnitude of $\Delta L/L_o$ was 95% of

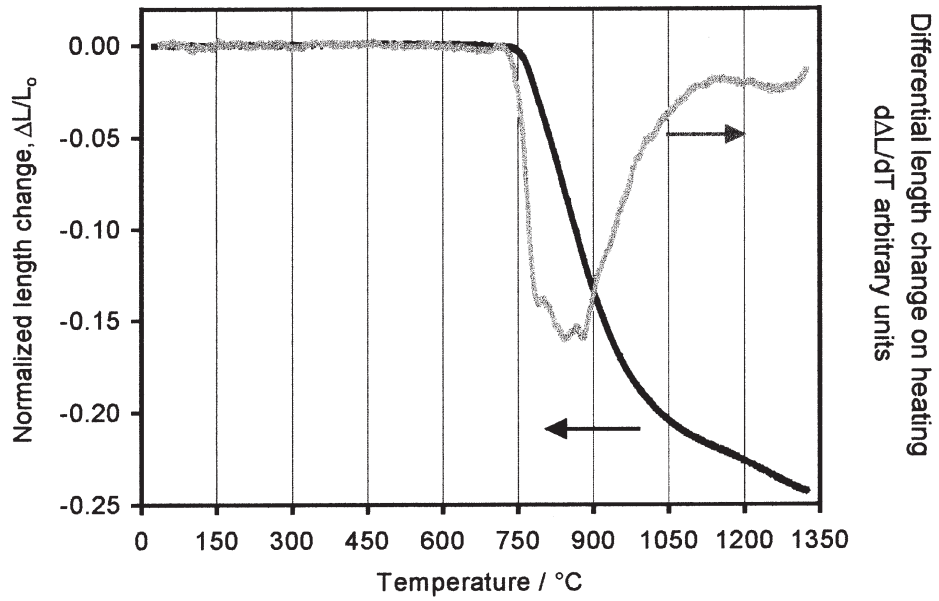

Fig. 3. Dilatometer curve (heating rate 3 °C min^{-1}) for a route 0 sample.

the maximum value) at 1100 °C and 980 °C respectively, compared with >1200 °C for the route 0 material.

Leite *et al.* [19] identified a maximum in the rate of linear shrinkage (minimum in the differential linear expansion) of a ZnO + Bi_2O_3 material at 771 °C (10 °C min^{-1} heating rate). The maximum was attributed to the formation of a bismuth-rich eutectic liquid [5]. Kim *et al.* [6] observed a similar maximum at 700–800 °C (5 °C min^{-1} heating rate) for a concentration of 1–10 at% Bi, but a shift in the maximum to ~900 °C for 0.02–0.2 at% Bi. In this study, local maxima were also

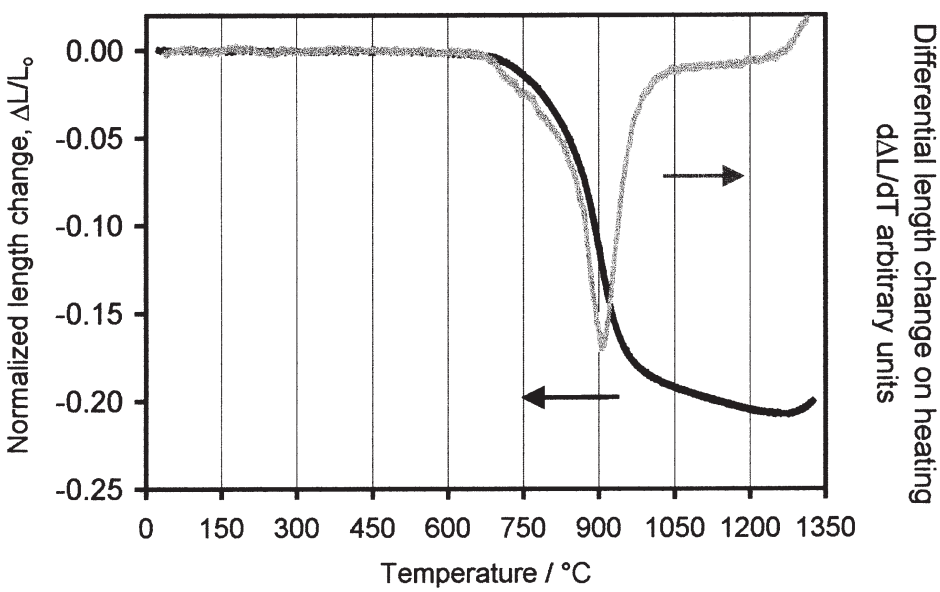

Fig. 4. Dilatometer curve (heating rate 3 °C min^{-1}) for a route 1 sample.

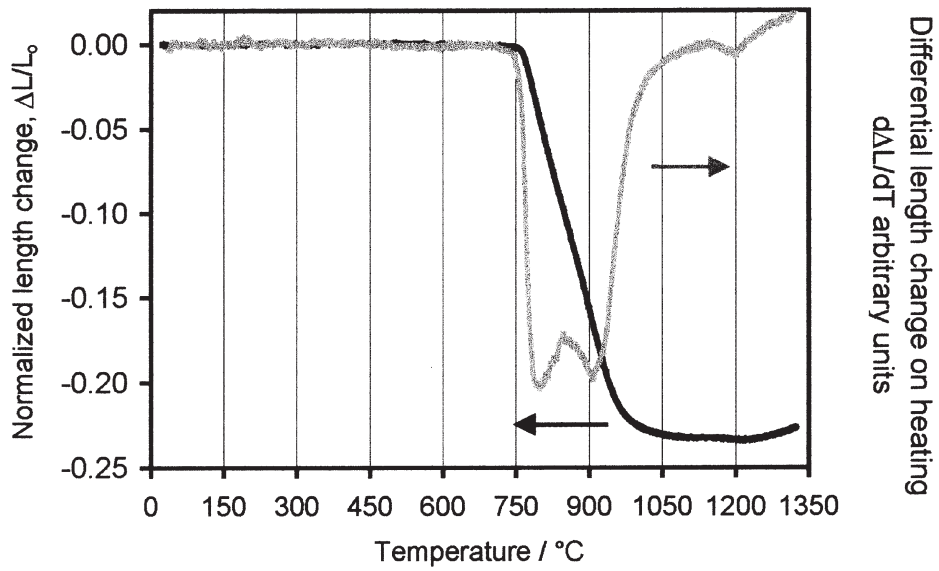

Fig. 5. Dilatometer curve (heating rate 3 °C min^{-1}) for a route 2 sample.

observed close to 770 °C for the green bodies from routes 0 and 2 (Figs. 3 and 5, respectively) which may be similarly attributed to the formation of a bismuth-rich liquid, whereas the route 1 green body showed only a single local maxima at 910 °C (Fig. 4).

A multicomponent ZBSCCM system (ZnO with Bi, Sb, Co, Cr, Mn minor components) was found to have a single maximum, at 1048 °C [19], from which it was deduced that the formation of the bismuth-rich liquid phase was inhibited by the other minor components. Similarly the formation of an extensive liquid phase in the route 1 material at 770 °C was also inhibited by the minor components. Because the route 1 and 2 green bodies densified at different temperatures it may be reasoned that the two strategies must have produced materials which differed in their local distributions of minor components. The most obvious and probable difference would have arisen from the incomplete diffusion of the dopants (Co, Mn, Al, Ni, Cr) into the ZnO grains under route 1. Hence, the local concentrations of dopants would be higher at the grain surfaces under route 1 than route 2 as shown schematically in Fig. 6.

The low surface concentration of dopants and high surface concentration of additives under route 2, and in localised regions of the green bodies under route 0, was suitable for the formation of a liquid phase at ~770 °C. A further densification process at ~910 °C was common to pellets from all three routes and may have involved the formation of a liquid phase contain-

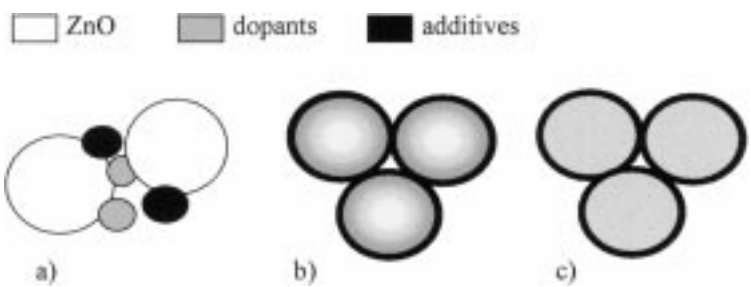

Fig. 6. Schematic representation of dopant and additive distributions in the green bodies prepared by a) route 0, b) route 1, c) route 2. Note that depth of grey shading indicates dopant concentration.

Table 3. Comparison of green and final density for the three synthetic routes

Sample	Synthesis route	Green density / % of theoretical maximum	Sinter density / % of theoretical maximum
P0	Route 0, mixed-oxide	58.0 ± 0.9	94.8 ± 1.3
P1	Route 1, precipitation	55.0 ± 0.9	95.7 ± 1.3
P2	Route 2, co-precipitation	50.2 ± 0.8	98.1 ± 1.3

ing both additives and dopants. Hence the route 1 powder would have densified primarily through the formation of a single liquid phase, whereas the route 2 powder underwent a two-stage densification. Densification of the route 0 powder proceeded through a number of steps (at least three) reflecting the large variations in the local dopant and additive concentrations arising from the precursor powders.

It may be noted from the sinter densities in Table 3 that under the normal sintering conditions (90 min sintering at 1000 °C) the bodies were almost completely dense. This would imply that incomplete densification in the dilatometer at 1000 °C, as revealed by the $\Delta L/L_o$ vs. T curves, for the route 0 and route 1 powders (Figs. 3 and 4, respectively) was a kinetic rather than thermal effect. Thus it may be reasoned that densification (at 1000 °C) occurred most rapidly for the powder prepared by route 2 and least rapidly for that prepared by route 0. From Table 3 the green bodies of samples derived by routes 1 and 2 had lower densities than those from the conventional route 0. After sintering, the densities of all three types of pellets increased. The sintered body densities increased in the order P0 < P1 < P2, as may have been expected from the more rapid densification of the novel materials.

Figs. 7 to 9 show SEM micrographs, with a BSE

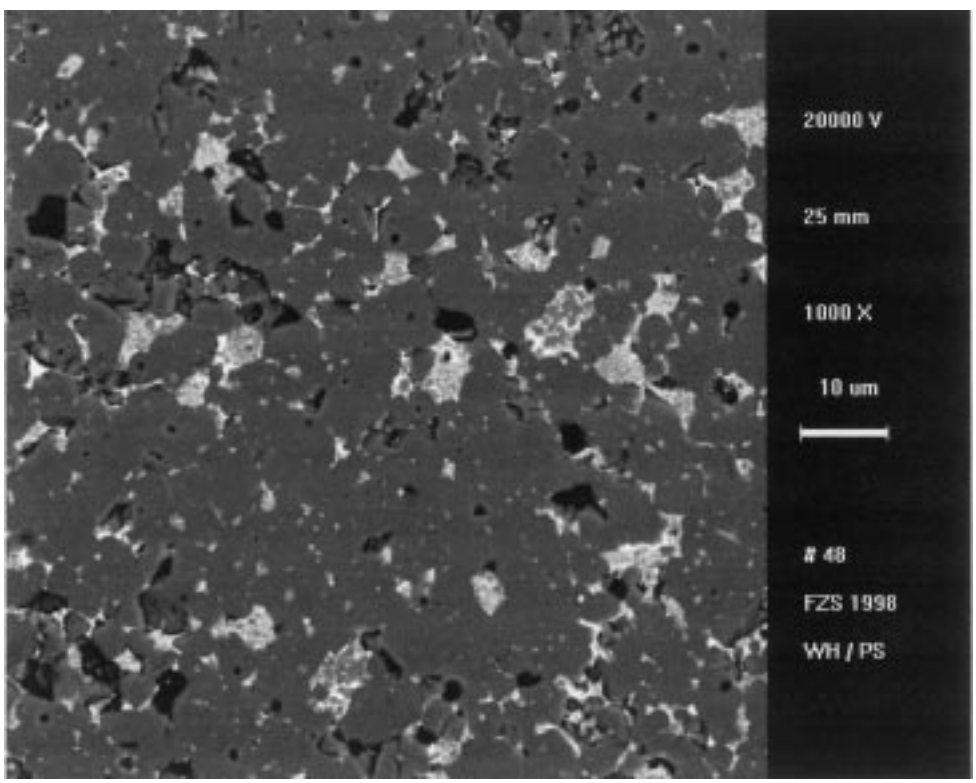

Fig. 7. Scanning electron micrograph for a P0 (route 0, sintered) sample, BSE detector

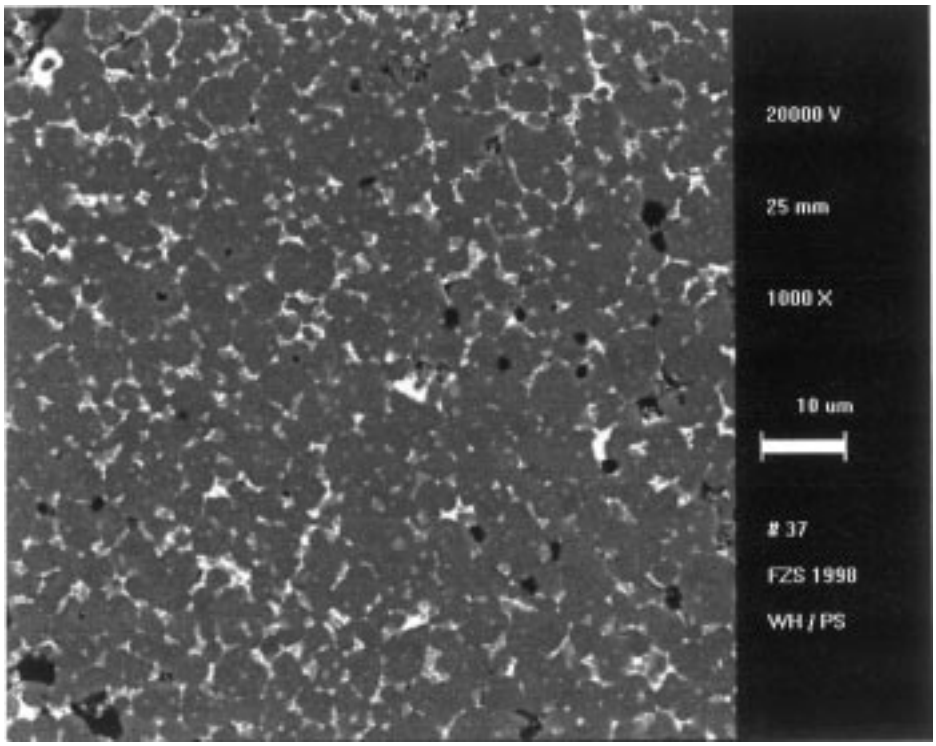

Fig. 8. Scanning electron micrograph for a P1 (route 1, sintered) sample, BSE detector

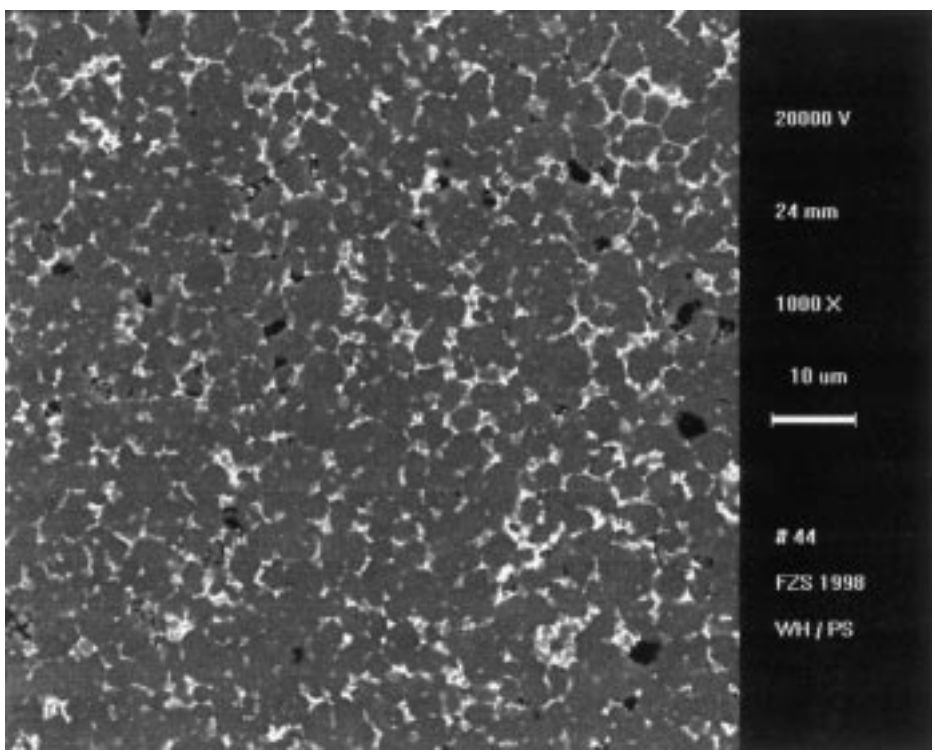

Fig. 9. Scanning electron micrograph for a P2 (route 2, sintered) sample, BSE detector

detector, of sintered, polished samples. In BSE micrographs at 20 KeV Bi_2O_3 appears white, spinel and pyrochlore light grey and the ZnO grains dark grey [20]. Black patches in the micrographs represent voids, which generally resulted from grains becoming dislodged during polishing. The micrographs of P1 and P2 (Figs. 8 and 9 respectively) show similar homogeneous distributions of the intergranular phases and ZnO grains. This is in contrast to P0 (Fig. 7) which shows a distinctly inhomogeneous distribution. In particular aggregates of intergranular material of ~4 μ diameter are clearly visible. Thus, some of the inhomogeneity of the starting materials is retained, even after sintering at 1000 °C.

Scanning electron micrographs, of the thermally etched samples, are given in Figs. 10 to 12. The boundaries between grains are more clearly visible than in the previous BSE images (Figs. 7 to 9).

Because there were many voids and some intergranular inclusions, it was decided to use an intercept method, in accordance with previous studies [21], in preference to an area technique to calculate the average grain size. The average intercept lengths, from >100 measurements per sample, were multiplied by 1.56 to obtain the average grain diameters [22]. By using this technique to analyse the SEM images of the etched samples (Figs. 10 to 12) it was found that the average grain sizes decreased in the order P0 > P1 > P2, with values of 7.4, 5.9 and 5.6 μm respectively. The similarity in grain size and microstructure of P1 and P2 is perhaps surprising, given the dilatometry measurements which indicate that P1 would have densified in a single stage and P2 in two. However, a more homogeneous distribution of spinel phases, which inhibit grain growth [19,23,24], in both the route 1 and route 2 pellets as compared with those from route 0 may explain the larger grain size of the conventional material.

4. Conclusions

Dense, doped ZnO ceramic pellets were produced by three different synthetic methods; conventional mixed-oxide, precipitation and co-precipitation citrate gel. The two non-conventional routes produced pre-

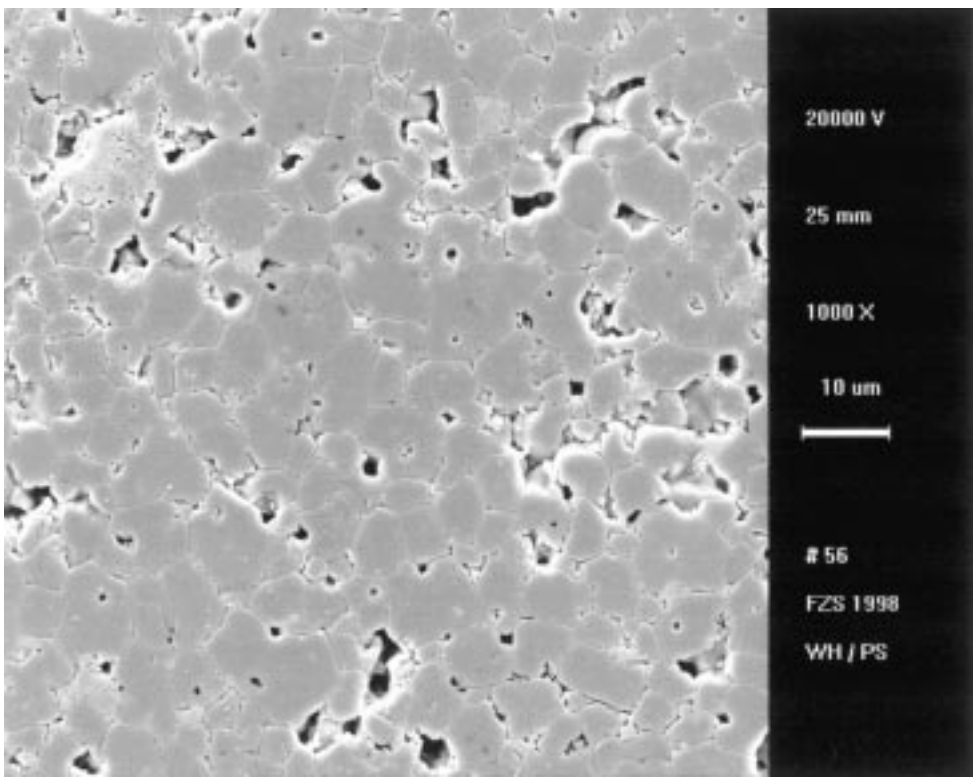

Fig. 10. Scanning electron micrograph for a P0 (route 0, sintered) sample after thermal etching, SE detector

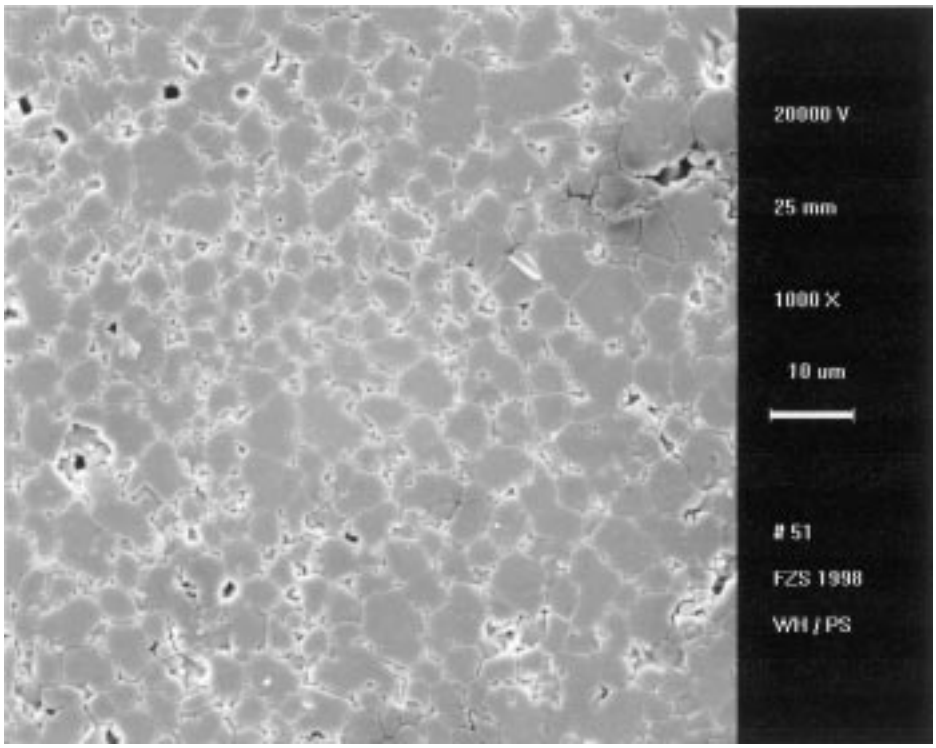

Fig. 11. Scanning electron micrograph for a P1 (route 1, sintered) sample after thermal etching, SE detector

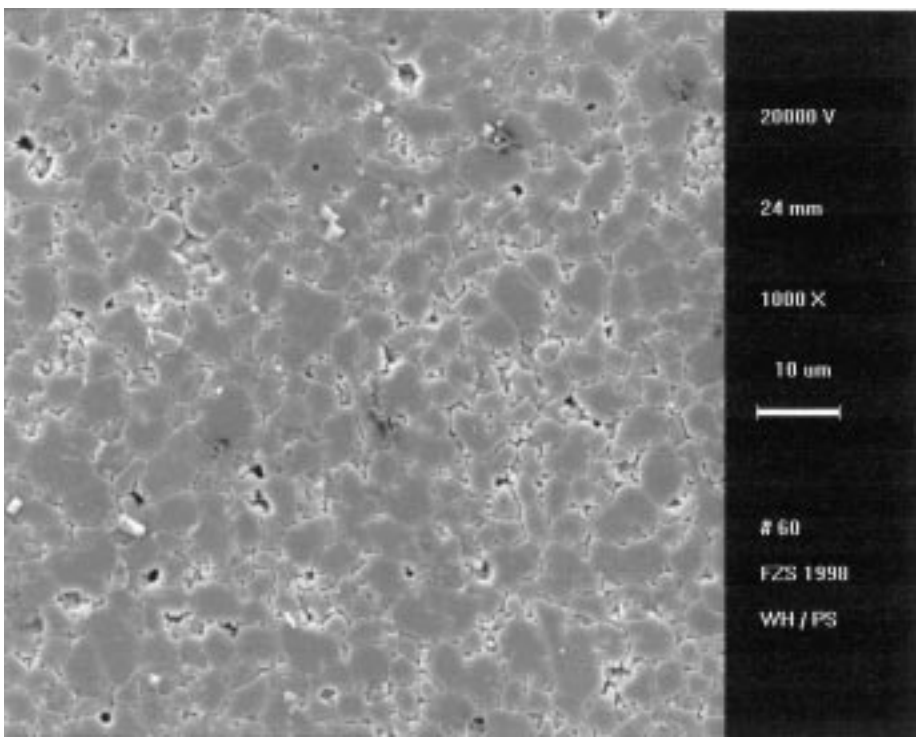

Fig. 12. Scanning electron micrograph for a P2 (route 2, sintered) sample after thermal etching, SE detector

cursor powders which sintered more readily and in fewer distinct stages (one or two compared with many) than a powder prepared by the conventional mixed-oxide route. This was attributed to the tailored microstructural variations in minor component concentrations for the novel routes compared with the random, inhomogeneous nature of the conventional, mixed-oxide material.

In addition SEM micrographs revealed that the novel routes led to pellets with smaller grains of doped ZnO and more homogeneously dispersed intergranular phases than the conventional synthesis, indicating that some of the green body microstructure was retained after sintering.

Acknowledgments

We thank Siemens-Matsushita, Deutschlandsberg (now EPCOS) for providing materials. Discussions with Prof. J. Schoonman are gratefully acknowledged.

References

1. T. K Gupta, *J. Am. Ceram. Soc.*, **73,** 1817 (1990).
2. E. Olsson, G. Dunlop, and R. Österlund, *J. Am. Ceram. Soc.*, **76,** 65 (1993).
3. J. Fan and F.R. Sale, in *Electroceramics: Production, Properties and Microstructures*, edited, *British Ceramic Proceedings 52*, W.E. Lee and A. Bell, eds. (The Institute of Materials, Ashgate Publishing Company, London, 1994) p. 151.
4. D. Dey and R.C. Bradt, *J. Am. Ceram. Soc.*, **75,** 2529 (1992).
5. T. Senda and R.C. Bradt, *J. Am. Ceram. Soc.*, **73,** 106 (1990).
6. J. Kim, T. Kimura, and T. Yamaguchi, *J. Am. Ceram. Soc.*, **72,** 1541 (1989).
7. T.K. Gupta, *J. Mater. Res.*, **7,** 3280 (1992).
8. M. Matsuoka, in *Advances in Ceramics 1*, L.M. Levinson, ed. (The American Ceramic Society, inc., Columbus, Ohio, 1981) p. 290.
9. P.N. Santhosh, H.S. Potdar, and S.K. Date, *J. Mater. Res.*, **12,** 326 (1997).
10. R.G. Dosch, B.A. Tuttle, and R.A. Brooks, *J. Mater. Res.*, **1,** 90 (1986).
11. S.M. Haile, D.W. Johnson Jr., G.H. Wiseman, and H.K. Bowen, *J. Am. Ceram. Soc.*, **72,** 2004 (1989).
12. G. Westin, A. Ekstrand, M. Nygren, R. Österlund, and P. Merkelbach, *J. Mater. Chem.*, **4,** 614 (1994).
13. A. Ekstrand, M. Nygren, and G. Westin, *J. Sol-Gel Sci. Tech.*, **8,** 697 (1997).
14. C. Marcilly, P. Courty, and B. Delmon, *J. Am. Ceram. Soc.*, **53,** 56 (1970).
15. D.J. Anderton and F.R. Sale, *Powder Metallurgy*, **1,** 14 (1979).
16. M.S.F. Baythoun and F.R. Sale, *J. Mater. Sci.*, **17,** 2757 (1982).
17. F.R. Sale and F. Mahloojchi, *Ceram. Int.*, **14,** 229 (1998).
18. F. Mahloojchi and F.R. Sale, *Ceram. Int.*, **15,** 51, (1989).
19. E.R. Leite, M.A.L. Nobre, E. Longo, and J.A. Varela, *J. Mater. Sci.*, **31,** 5391 (1996).
20. F. Greuter, T. Christen, and J. Glatz-Reichenbach, *Mat. Res. Soc. Symp. Proc.*, **500,** 235 (1998).
21. Y.S. Lee and T.Y. Tseng, *J. Mater. Sci.*, **8,** 115 (1997).
22. M.I. Mendelson, *J. Am. Ceram. Soc.*, **52,** 443 (1969).
23. E. Olsson, L.K. Falk, and G.L. Dunlop, *J. Mater. Sci.*, **20,** 4091 (1985).
24. J. Wong, *J. Appl. Phys.*, **46,** 1653 (1975).